Flight Tests of Tow Wire Forces while Flying a Racetrack Pattern

C. Matuk*
University of Luleå, Luleå, Sweden

Airplane towing of a target with a long wire in a racetrack pattern has been investigated. First the theoretical background is presented and then the experiments are treated. Twelve flights with different airplane speeds and turn radii are studied. The force at the airplane end of the wire, and the airplane and the target paths are plotted. The maximum force in the wire occurs after the airplane turn is finished. This maximum value is due to whip effect. The occurrence of maximum and minimum values for the vertical distance between airplane and target is demonstrated. The experimental results are compared with theoretical results for the conditions of the experiments. The overall agreement is considered satisfactory. Therefore theoretical graphs on the maximum force in the wire as a function of airplane speed and turn radius can be used to avoid wire failure while flying a racetrack pattern.

Nomenclature

A,B,C,D	= points in graphs used to indicate the beginning or the end of events (with subscripts P or T or without subscripts)
A_m	= projected area of the target
C_d	= drag coefficient for the wire
C_l	= lift coefficient for the wire
C_m	= drag coefficient for the target
$\boldsymbol{e}_d$, $\boldsymbol{e}_l$	= unit vectors
F	= force at the airplane end of the wire
$\boldsymbol{G}$	= acceleration of gravity vector
H	= vertical distance between airplane and target
K	= total kinetic energy
L	= wire length
m	= target mass
$\boldsymbol{P}(s,t)$	= vector position of the wire
$\boldsymbol{P}_m(t)$	= vector position of the target
$\boldsymbol{P}_P(t)$	= vector position of the airplane end of the wire
R	= turn radius
s	= wire coordinate
t	= time
V	= airplane speed
α	= angle between the wire and the velocity vector
δW	= total virtual work
$\delta W_S, \delta W_d, \delta W_l, \delta W_g, \delta W_f$	= partial virtual works
ρ	= wire density
ρ_a	= air density
σ	= wire stress vector
σ_u	= ultimate strength
ϕ	= wire diameter

Subscripts

max	= maximum value
min	= minimum value
0	= straight flight conditions
P	= for the airplane
T	= for the target

Introduction

SAFETY stipulations for airplanes require long wires for target towing at high speeds. Wire failure occurs sometimes when the airplane flies a racetrack pattern. The stress in the wire reaches the ultimate strength due to whip effect. Therefore it is necessary to predict the maximum stress or force in the wire.

A theoretical study on airplane towing of a target in a racetrack pattern was presented by Matuk.[1] Experimental investigations on racetrack patterns have not been found in the literature. Experimental studies of target towing during straight airplane flights have been presented by several authors, for example, Bragg et al.[2] and Bartlett.[3] Matuk[4] made a theoretical investigation of towing for rectilinear airplane accelerations.

This paper presents first a review of the theoretical background and then experiments on airplane towing of a target in a racetrack pattern. Theoretical results from Ref. 1 were used to plan the flights. The force at the airplane end of the wire as a function of time is obtained in the experiments. Also, vertical positions of airplane and target as functions of time, and horizontal views of airplane and target paths are presented. Comparison between experiments and theory is made for the maximum force in the wire and for the vertical distance between airplane and target.

Theoretical Background

Consider the model for a wire and a target shown in Fig. 1. The wire is characterized by its length L, diameter ϕ, and density ρ, and finally, by its Kelvin material. The target is characterized by its mass m and its projected area A_m in a plane perpendicular to the relative velocity between the surrounding air and the target. The air is represented by its density ρ_a, the drag coefficient C_d, and the lift coefficient C_l for the wire, and finally, by the drag coefficient C_m for the target. Gravity is characterized by the acceleration vector $\boldsymbol{G}$.

A reference frame moving with the constant velocity of the air is defined. s is the material coordinate along the wire (see Fig. 1). At time t the position of wire section s is $\boldsymbol{P}(s,t)$. If K denotes the kinetic energy and W the virtual work of the wire and the target, the extended Hamilton's principle can be expressed

$$\delta\int_{t_1}^{t_2} K\mathrm{d}t+\int_{t_1}^{t_2}\delta W\mathrm{d}t=0 \tag{1}$$

The kinetic energy K is

$$K=m\left|\frac{\partial \boldsymbol{P}_m}{\partial t}\right|^2/2+\int_{s=0}^{L}\rho\frac{\pi\phi^2}{4}\left|\frac{\partial \boldsymbol{P}}{\partial t}\right|^2\mathrm{d}s/2 \tag{2}$$

Received March 15, 1982; revision received Sept. 7, 1982.

*Department of Mechanical Engineering.

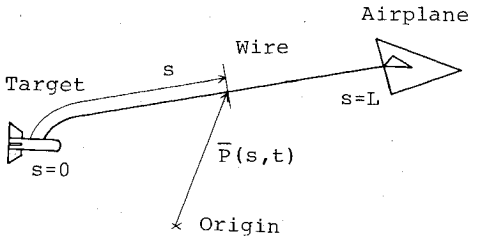

Fig. 1 Model of a towing system with wire coordinate s and vector position $P(s,t)$.

where $\boldsymbol{P}_m(t)$ denotes the position of the target. The increment of virtual work δW is

$$\delta W=\delta W_S+\delta W_d+\delta W_l+\delta W_g+\delta W_f \tag{3}$$

δW_S is the contribution due to the stress in the wire. δW_d is due to the drag force on the wire and the target, and δW_l is due to the lift force on the wire. Gravity contributes with δW_g. δW_f is due to the force $\boldsymbol{F}$ between wire and airplane.

The virtual work δW_S due to the stress in the wire is

$$\delta W_S=\int_{s=0}^{L}\left(\frac{\pi\phi^2}{4}\right)\left(\frac{\partial\sigma}{\partial s}\right)\mathrm{d}s\cdot\delta\boldsymbol{P} \tag{4a}$$

where σ is the stress vector due to small strains in the Kelvin material of the wire. The virtual work δW_d due to the drag forces on the wire and the target can be expressed

$$\delta W_d=C_m A_m\rho_a\left(\left|\frac{\partial\boldsymbol{P}_m}{\partial t}\right|^2/2\right)\boldsymbol{e}_d\cdot\delta\boldsymbol{P}_m$$

$$+\int_{s=0}^{L}C_d\phi\rho_a\left(\left|\frac{\partial\boldsymbol{P}}{\partial t}\right|^2/2\right)\boldsymbol{e}_d\mathrm{d}s\cdot\delta\boldsymbol{P} \tag{4b}$$

where $\boldsymbol{e}_d$ is a unit vector in the direction of the drag forces. The virtual work δW_l due to the lift forces on the wire is

$$\delta W_l=\int_{s=0}^{L}C_l\phi\rho_a\left(\left|\frac{\partial\boldsymbol{P}}{\partial t}\right|^2/2\right)\boldsymbol{e}_l\mathrm{d}s\cdot\delta\boldsymbol{P} \tag{4c}$$

where $\boldsymbol{e}_l$ is a unit vector in the direction of the lift forces. The drag and lift coefficients used for the wire are respectively $C_d=0.02+1.1\sin^3\alpha$ and $C_l=1.1\sin^2\alpha\cos\alpha$. α is the angle between a tangent to the wire at a particular wire coordinate and the wire velocity vector at the same wire coordinate. The virtual work δW_g due to gravity on the wire and target can be expressed

$$\delta W_g=m\boldsymbol{G}\cdot\delta\boldsymbol{P}_m+\int_{s=0}^{L}\rho(\pi\phi^2/4)\boldsymbol{G}\mathrm{d}s\cdot\delta\boldsymbol{P} \tag{4d}$$

Finally, the virtual work δW_f due to the force $\boldsymbol{F}$ between the wire and the airplane is

$$\delta W_f=\boldsymbol{F}\cdot\delta\boldsymbol{P}_P \tag{4e}$$

where $\boldsymbol{P}_P$ is the position of the airplane end of the wire. The motion of this end shall be prescribed.

Replacement of Eqs. (2-4) into Eq. (1) gives a variational equation containing second-order partial derivatives in wire coordinate and in time. This equation cannot be solved analytically. Therefore discretization is performed first along the wire and then in time.

Division of the wire into segments of equal length is considered. Discretization along the wire is achieved by symmetrical replacement of functions with mean values and of wire coordinate derivatives with central differences. Thus a discretized version of the extended Hamilton's principle is obtained, from which Lagrange's equations are derived. These equations are nonlinear ordinary differential equations of the second order in time and do not allow an analytical solution. Therefore discretization in time is performed by replacement of time derivatives with central differences.

A Fortran computer program solves the equations to obtain the position of the wire and the stress along it. The motion of the airplane end of the wire shall follow a racetrack pattern.

The details of this theory are presented in Ref. 1.

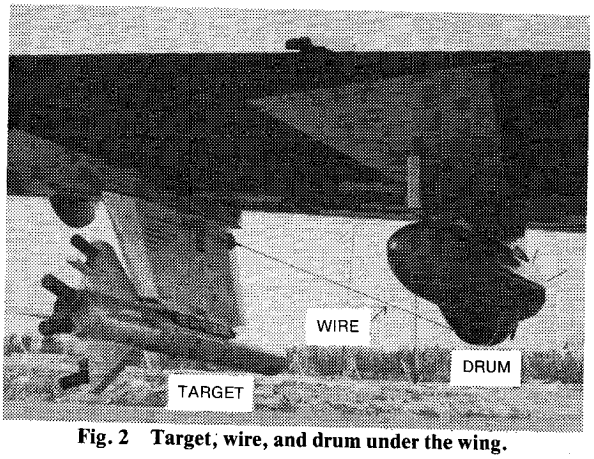

Fig. 2 Target, wire, and drum under the wing.

Experimental Procedure

The target and the wire used in the flights are shown in Fig. 2. They were located under one of the airplane wings. The wire passes from a drum through a launch mechanism to the target. The wire was made of music steel with diameter $\phi=1.3$ mm and ultimate strength $\sigma_u=2450$ MPa. The drum was blocked when the wire reached a length of $L=5$ km. The target has mass $m=28$ kg, cross-sectional area of central body and wings $A_m=0.06\ \mathrm{m}^2$, and drag coefficient $C_m=0.35$.

A stiff spring was placed between the target and the wire. Another stiff spring supported a pulley in the launch mechanism. This last spring can be considered as located between the wire and the airplane, when the drum is blocked. The springs were so stiff that they did not influence the motion of the target or the force in the wire, as demonstrated in Ref. 1. This reference showed also that the force in the wire reached a maximum at the airplane end of the wire. Therefore the force F at the airplane end of the wire as a function of time was measured by a force gage on a pulley in the launch mechanism. This force was recorded in the airplane. The accuracy of the measurements was ± 50 N.

In the racetrack pattern the airplane should first fly in a straight path, then make a semicircular turn, and finally fly again in a straight path, all at the constant altitude of 4 km. Each flight should have constant airplane speed V and constant turn radius R, both with respect to the surrounding air (the speed indicator in the airplane indicated the airplane speed with respect to the air). The straight airplane path before the turn should be aligned in the direction of the wind. This simplifies later calculations based on graphs of the airplane and target paths.

During the flights one radar station followed the airplane and another followed the target. Each radar had at least ± 50 m accuracy for the first measured position of the airplane or the target according to the instrument specifications. The positions following the first position are measured with ± 10 m accuracy with respect to the first position. Therefore the error in the airplane or target altitude is dominated by the error of the first measured position. The radar measurements showed that the airplane speed with respect to the ground, and the airplane altitude varied slightly. Also, the airplane

velocity before the turn deviated slightly from the direction of the wind.

Consider the airplane velocities with respect to the ground in the straight paths before and after the semicircular turn. Half the difference between these velocities gives the airplane speed V with respect to the air, and half the sum gives the wind speed with respect to the ground. The deviation between the straight airplane path and the wind velocity gives less than 0.5% error in calculating the airplane speed V with respect to the air. Also the wind velocity was measured before and after the flights. The wind speed was between 50 and 70 km/h.

Radio communication between the airplane and the ground station was maintained during each flight. This was necessary to synchronize events between the force measured in the airplane and the airplane and target positions measured at the ground station. The radar measurements of position and velocity for the airplane and the target, and the radio communication were recorded.

Twelve flights with different airplane speeds and turn radii were performed. The flight with airplane speed $V = 562$ km/h and turn radius $R = 1.7$ km shall be considered as a representative flight.

Experimental Results

Graphs on the force at the airplane end of the wire and on the positions of the airplane and the target for the representative flight are presented in Fig. 3. In the figure the points A indicate the beginning of the recorded airplane and target paths, and the points B indicate the beginning of the airplane turn. The points C indicate the beginning of the final straight path after the airplane turn, and the points D indicate the end of the recorded airplane and target paths.

The force F at the airplane end of the wire as a function of time is shown in Fig. 3a. It should be noticed that the maximum force F_{max} due to a whip effect occurs after the airplane turn is finished (point C). Also, it is seen that the force peak is rapidly damped by the air.

A horizontal view of the airplane and the target paths with respect to the ground is shown in Fig. 3b. The airplane and the target paths for the straight flight A-B do not coincide because the airplane velocity before the turn deviated slightly from the direction of the wind. The section B_P-C_P of the airplane path is not semicircular in the figure because of the presence of wind. However, it is close to semicircular with respect to the air. The value of the turn radius R with respect to the air is obtained directly from Fig. 3b.

The vertical positions of airplane and target as functions of time are presented in Fig. 3c. A mean airplane altitude was

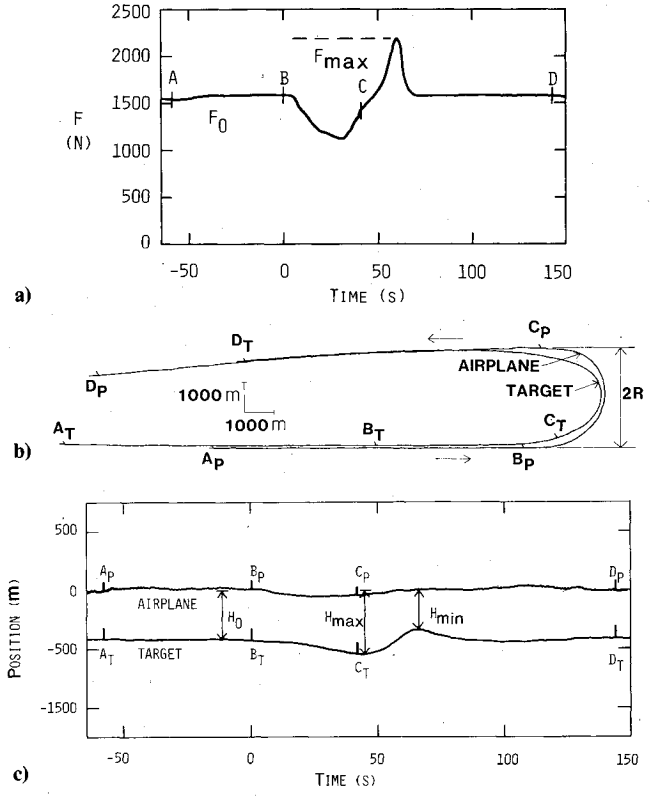

Fig. 3 a) Force at the airplane end of the wire as a function of time for the representative flight. b) Horizontal view of airplane and target paths for the representative flight. c) Vertical positions of airplane and target as functions of time for the representative flight.

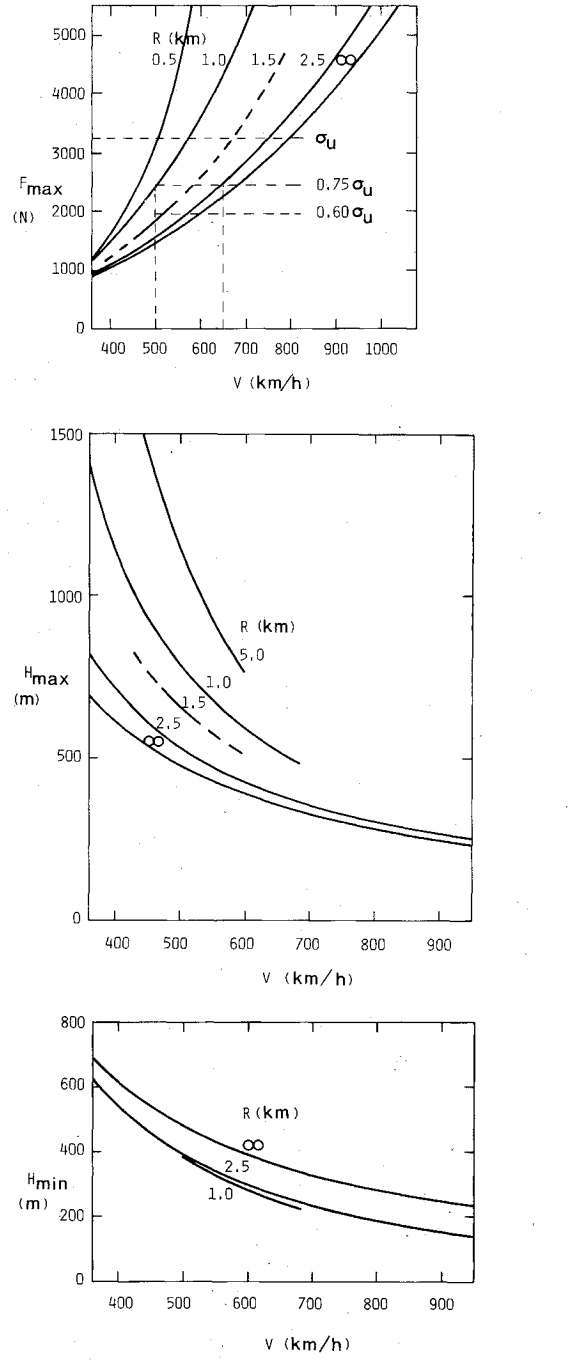

Fig. 4 a) Theoretical maximum force in the wire F_{max} as a function of airplane speed V and turn radius R. b) Theoretical maximum vertical distance between airplane and target H_{max} as a function of airplane speed V and turn radius R. c) Theoretical minimum vertical distance between airplane and target H_{min} as a function of airplane speed V and turn radius R.

Table 1 Forces in the wire F_0 and F_{max} for the different flights

Flights V, km/h	R, km	F_0,N Experiment	Theory	Deviation, %	F_{max},N Experiment	Theory	Deviation, %
650	3.0	1900	2250	−16	2000	2400	−17
643	3.0	1850	2250	−18	2000	2400	−17
623	2.6	1750	2100	−17	1950	2250	−13
617	2.3	1750	2100	−17	2000	2400	−17
567	1.6	1600	1800	−11	2250	2300	−2
562	1.7	1600	1750	−9	2200	2200	0
563	2.4	1600	1750	−9	1700	1900	−11
560	2.6	1550	1750	−11	1700	1900	−11
524	2.0	1500	1550	−3	1650	1800	−8
522	1.9	1450	1550	−6	1700	1800	−6
500	1.8	1400	1450	−3	1650	1700	−3
499	1.7	1400	1450	−3	...	1700	...

Table 2 Vertical distances between airplane and target H_0, H_{max}, and H_{min} for the different flights

Flights V, km/h	R, km	H_0,m Experiment	Theory	Deviation, %	H_{max},m Experiment	Theory	Deviation, %	H_{min}, m Experiment	Theory	Deviation, %
650	3.0	338	358	−6	350	380	−8	260	275	−5
643	3.0	353	364	−3	363	386	−6	200	278	−28
623	2.6	375	376	0	408	406	0	198	285	−31
617	2.3	368	380	−3	450	416	8	248	282	−12
567	1.6	395	417	−5	588	527	12	350	315	11
562	1.7	420	420	0	540	519	4	335	320	5
563	2.4	415	419	−1	453	464	−2	283	330	−14
560	2.6	405	422	−4	458	460	0	315	332	−5
524	2.0	493	454	9	550	545	1	345	365	−5
522	1.9	490	457	7	623	556	12	328	365	−10
500	1.8	495	478	4	640	600	7	328	390	−16
499	1.7	495	479	3	648	605	7	383	390	−2

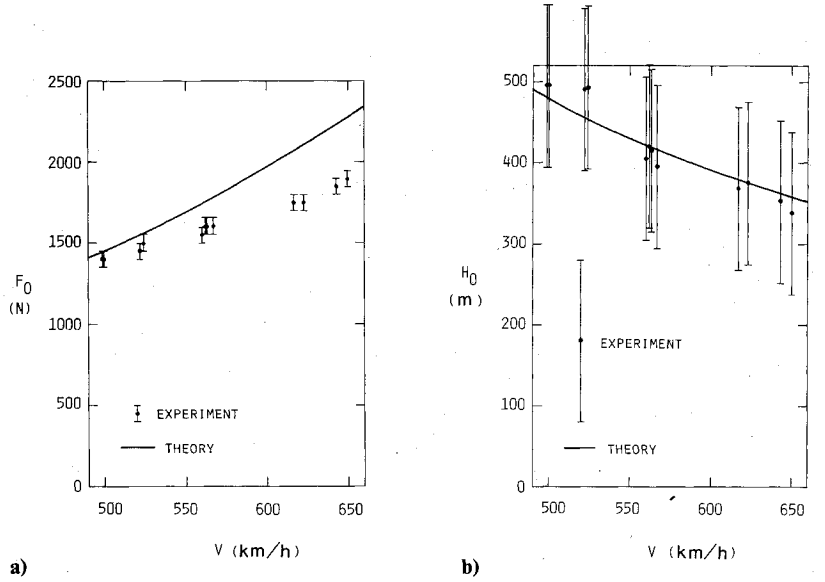

Fig. 5 a) Comparison of experimental and theoretical force in the wire during straight flight. b) Comparison of experimental and theoretical vertical distance between airplane and target during straight flight.

calculated using 18 equally spaced points between A_P and D_P. The zero level of the vertical scale in Fig. 3c is located at this mean airplane altitude. Vertical distances between airplane and target are determined from this mean airplane altitude. A mean target altitude during straight flight was obtained as a mean value of four different target altitudes. Three of them were taken at points A_T, B_T, D_T, and the fourth was taken halfway between A_T and B_T. Notice that the maximum vertical distance H_{max} and the minimum vertical distance H_{min} occur after the airplane turn is finished.

Diagrams of the same type as in Fig. 3 were obtained for the 12 flights.

Comparison Between Experiments and Theory

Theoretical forces in the wire and theoretical airplane and target positions can be obtained using the theory presented in the beginning of this paper. For the conditions of the experiments, the theoretical maximum force F_{max} as a function of airplane speed V and turn radius R was obtained and is shown in Fig. 4a. The dashed part of the curve for the turn radius $R = 1.5$ km represents extrapolated values. This figure was used to plan the first six flights for a theoretical maximum force corresponding to about 60% of the ultimate strength for the wire. The remaining six flights were planned

for 75% of the ultimate strength. These force levels are indicated in the figure. It should be noticed that a turn radius $R = \infty$ represents straight flight.

A comparison between experiments and theory is presented in Tables 1 and 2. The 12 flights are organized in decreasing speed. Experimental and theoretical forces in the wire F_0 and F_{max} and the percentual deviation between experiments and theory are given in Table 1. The theoretical values were obtained by interpolation between curves in Fig. 4a. Table 2 gives the vertical distances between airplane and target H_0, H_{max}, and H_{min} for the different flights. The theoretical values were obtained by interpolation from Figs. 4b and 4c. The overall agreement between experiments and theory is considered satisfactory.

The deviation between experiments and theory for the forces in the wire F_0 and F_{max} in Table 1 is less than 19%. It should be noticed that the experimental forces are smaller than the theoretical. The deviation for the vertical distances between airplane and target H_0 and H_{max} in Table 2 is less than 13%. A larger deviation for the forces than for the vertical distances is expected, as in the theory the forces are derived from differences between positions. One reason for the deviation between experiments and theory is the simplifying assumptions behind the theoretical model. Another reason for the deviation is the restrictions in the computer program used in the theory. The computer program does not permit variations in the airplane speed, turn radius, or airplane altitude as occurred in the experiments.

Theoretical and experimental values for the force in the wire F_0 and for the vertical distance H_0 during straight flight, as functions of the airplane speed V, are shown graphically in Fig. 5. The vertical straight lines through the experimental points represent maximum errors. The agreement between the experimental and theoretical vertical distances H_0 in Fig. 5b is good. This suggests a real accuracy much better than that indicated in the figure, which is based on the instrument specifications.

Conclusions

The experiments show that the maximum force at the airplane end of the wire occurs after the airplane turn is finished. This maximum force is due to whip effect. The occurrence of marked maximum and minimum values for the vertical distance between airplane and target is also shown by the experiments.

The overall agreement between experiments and theory is considered satisfactory.

The experiments gave a force in the wire smaller than the theoretical force. Therefore the theoretical maximum force in the wire, presented in the previous section, is conservative when used to avoid wire failure while flying racetrack patterns with semicircular turns.

Acknowledgment

This investigation was supported by the Swedish Defense Material Administration (FMV).

References

[1]Matuk, C., "Stress in a Viscoelastic Towing Wire with End Dampers due to an Airplane Turn," *Transactions of the Canadian Society for Mechanical Engineering,* Vol. 6, No. 4, 1980-81, pp. 220-225.

[2]Bragg, P., Cripps, T.P., and Grieve, B.S., "Meteor TT Mk.20—Performance and Handling Trials with a Rushton Towed Target System," AAEE/817/6, Part 4, Great Britain Aeroplane and Armament Experimental Establishment, Boscombe Down, Amesbury, Wilts, England, 1966.

[3]Bartlett, W.L., "Drag and Compatibility Test of the TDU-4/B Target with the B57E External Lightweight Tow System," APGC-TR-59-39, Air Proving Ground Center, Eglin Air Force Base, Fla., 1959.

[4]Matuk, C., "Dynamic Stress in a Towing Wire due to Forced Acceleration," *Journal of Aircraft,* Vol. 18, June 1981, pp. 498-499.